

Configuration of 3U CubeSat Structures for Gain Improvement of S-band Antennas

Vivek Shirvante, Shawn Johnson, Kathryn Cason, Kunal Patankar
 Norman G. Fitz-Coy
 University of Florida, Space Systems Group
 187 Engineering Building, Building 33 Gainesville, FL 32612; (352) 846-3020
 itsviv311@ufl.edu

ABSTRACT

Nano- and pico-satellites in low earth orbit (LEO), unlike their larger counterparts, have more stringent limitations on antenna design due to power constraints that govern the operational frequency and size that defines the mass and volume constraints. High bandwidth applications use higher frequencies and require higher transmission power. High gain antennas can reduce the transmission power requirements. CubeSat's with body-mounted solar cells are limited in power generation due to limited surface area. Deployable solar panels offer a solution to the limited power by maximizing the surface area of solar cells exposed to solar radiation. The metallic deployable solar panel support structure can be exploited to behave as an electrical ground and microwave signal reflector for a high gain antenna in several configurations. This paper presents multiple novel high-gain S-band antennas that exploit the structure of a 3U CubeSat equipped with deployable solar panels for gain improvement. The configuration of the satellite is designed to operate in a low drag configuration by operating outside of the passive gravity gradient stabilized attitude by using passive or active attitude control. Gain improvements of more than 3 dB are obtained through careful packaging. The antenna configurations have a gain of more than 7dBi and bandwidth of more than 10MHz. Analysis is provided with considerations of power, satellite coverage, as well as attitude stability. This technique of improving antenna gain can be extended to higher as well as lower frequency of operation.

INTRODUCTION

Reduced cost, rapid development time and the availability of small form factor attitude control systems has paved the way for high-utility applications of CubeSats such as fire detection, animal tracking and weather monitoring.¹ However, this new mission applications impose a heavier demand on the communication subsystem. For example, fire detection requires high resolution imaging of specific geographic areas and hence increases the bandwidth requirement for the communication downlink.

Bandwidth-intensive applications motivate the need for higher frequency communications downlink.² The S-band frequency spectrum, ranging from 2.2GHz to 2.3GHz as defined by the Federal Communications Commission (FCC), is one such frequency band that can be used for such applications.² Studies have been performed on the use of S-band communication capabilities of 3U CubeSats.⁶ However, higher frequencies are subject to higher path loss. Thus, to maintain a good communication link, higher transmission power is required.

High resolution imaging through CubeSats requires a high-precision attitude determination and control system (ADCS) with up to a few arc-sec precision.¹ Additionally, these systems contain other power-hungry hardware such as dedicated image-processing units and

high resolution imaging equipment. This high power demand coupled with the surface area constraint imposed by the CubeSat form factor inhibits the possibility of sufficiently increasing the transmission power to meet the demands on the communication downlink. Friss' free-space path loss equation shows that the transmission power for S-band communication can be reduced by employing high gain antennas.² Designing high gain antennas for a size constrained 3U CubeSat is challenging and with increased antenna directivity (gain) it is necessary to have higher attitude control system to maintain reliable communication link. Fortunately, recent advances in small form factor active attitude control systems makes it possible to use high-gain directional antennas on CubeSats to minimize communication link quality degradation due to pointing accuracy loss associated with such antennas.

Basic analysis shows that 3U CubeSats employing deployable solar panels are capable of generating up to 30W of power. The deployable solar panels metallic mounting structure can be exploited to achieve higher antenna gains through smarter packaging without necessitating the need for complex antenna designs.

Satellite ground coverage reduces with increased antenna gain. Thus the antenna design should be such that the gain is sufficient to meet the required link quality and coverage. In this paper a novel concept for

high gain antenna design that exploits the structure of a 3U CubeSat equipped with deployable solar panels and designed to be in a low drag configuration by operating outside of the passive gravity gradient attitude using active attitude control is presented.

APPROACH

Utilizing some of the possible deployable solar panel configurations, several S-band antenna designs are developed for gain values derived from detailed link budget analysis through consideration of power and footprint. Analysis is performed to evaluate satellite coverage and attitude stability.

To evaluate the characteristics of each antenna design, the ANSYS HFSS 3D electromagnetic simulation tool computes the gain, beam width and impedance. Mock configurations of the antennas are developed to evaluate the antenna impedance and improvement of received signal strength due to increased gain. Tests are then performed on antenna prototypes using an S-band transceiver and HP Agilent Vector Network Analyzer (VNA) HP8720ES. It is shown that the mission utility of each design is dictated by the mission requirement and the design concepts described can be extended to higher frequencies and other CubeSat form factors.

COMMUNICATION LINK BUDGET

Image transmission over a wireless channel is a bandwidth-intensive process requiring higher transmission power than typical CubeSat missions. High-resolution images captured for applications like fire detection are shown to require about 33Mbits of information per image.¹ If QPSK modulation scheme is assumed, then the required transmission bandwidth is 33MHz. Such high bandwidth is difficult to achieve due to system complexities at higher frequencies. Hence, the data should be transmitted with lower data rates. For the antenna design developed in this paper a bandwidth of 10MHz is considered.

Image transmission requires a lower bit error rate (BER) and hence the sensitivity (S) requirement for the receiver increases such that⁴

$$P_r = 10 \log(kT_{sys}BF) + SNR \quad (1)$$

where k = Boltzmann constant; T_{sys} = system noise temperature; SNR = signal-to-noise ratio (9.2dB for QPSK modulation scheme with bit error rate of 10^{-6}); B = bandwidth (10MHz); and F = noise factor (1.5).

The system noise temperature is given in by⁴

$$T_{antenna} = 10^{-a/10} T_{ant} + (1 - 10^{-a/10}) T_l \quad (2)$$

and

$$T_{sys} = T_{antenna} + (F - 1)T_0 \quad (3)$$

where T_{ant} =Antenna noise temperature (150K); T_0 =room temperature (300K); T_l = transmission line and connector loss temperature (290K); a = connector loss (1dB); F = noise factor (2dB); and T_{sys} = System noise temperature.

The antenna noise temperature is assumed to be 150K. Taking all these parameters into consideration, the required receiver sensitivity to achieve a data rate of 10Mbps is approximately -121.5dB. Thus the received signal strength should be a minimum of -121.5dB to obtain 10MHz bandwidth.

Friss' free-space path loss in Eq. (4) shows that the received signal power (P_r) is governed by transmission power (P_t) of 1W (0 dB), distance (R) of 500km, transmitter antenna gain (G_t), receiver antenna gain (G_r), atmospheric loss (A) of 3dB, polarization mismatch loss (P) of 2dB, reflection coefficient (γ) of -20dB and 13cm wavelength of signal at 2.3GHz (λ).³ A sensitivity of -121.5dB can be attained through careful selection of antenna gain.

$$P_r = 10 \log \left\{ P_t G_t G_r \left(\frac{\lambda}{4\pi R} \right)^2 \right\} \quad (4)$$

The ground station is assumed to use an S-band parabolic dish antenna with a 2m diameter (D), working at 2.3GHz frequency (f), and with an aperture efficiency (η) of 55%. The gain G_r of the antenna is 30.8dB where c is speed of light.⁵

$$G_r = 10 \log \left\{ \eta \left(\frac{\pi D f}{c} \right)^2 \right\} \quad (5)$$

For a low earth orbit satellite's communication link, the distance (h) between the satellite and ground station varies due to orbital motion. This motion leads to non-uniform strength of received signals due to path length variations. Given the parameters of elevation angle (ϵ), nadir angle (ϑ), radius of Earth (R_e), Earth central angle (Ψ), the variation in path with elevation (d) can be evaluated.²

$$\vartheta = \frac{\pi}{2} - \epsilon - \Psi \quad (6)$$

$$\vartheta = \arccos \left(\frac{R_e}{r} \cos \epsilon \right) \quad (7)$$

$$\epsilon = \arccos \left(\frac{r}{R_e} \sin \vartheta \right) \quad (8)$$

$$d = \sqrt{R_e^2 + r^2 - 2 R_e r \cos \vartheta} \quad (9)$$

Excluding the transmit antenna gain, the path loss variation with elevation angle is shown in Figure 2. It shows about 2dB difference between path loss at zenith and at elevation of 60 degrees leading to power fluctuation at receiver. If the elevation angle for a good communication link is set to 60 degrees, then the path loss obtained is about -128dB, which is 6.5dB lower than the sensitivity requirement of 121.5dB obtained earlier. At zenith the loss is 4.5dB lower than the sensitivity requirement. To compensate for this variation, the antenna gain should be increased, as an increase in transmission power is not an option for CubeSats. Thus, the antenna radiation pattern should have a minimum beam-width of 60 degrees, such that the corresponding gain at 60 degrees elevation angle is more than 6.5dB.

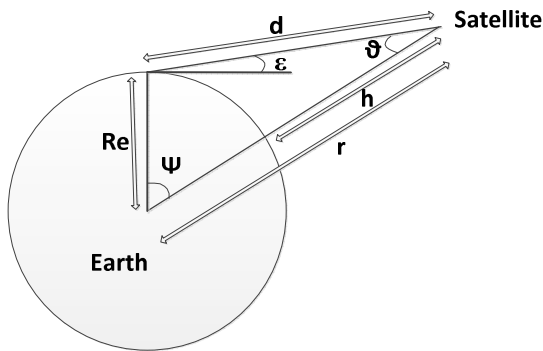


Figure 1: Geometric Representation of Slant Distance

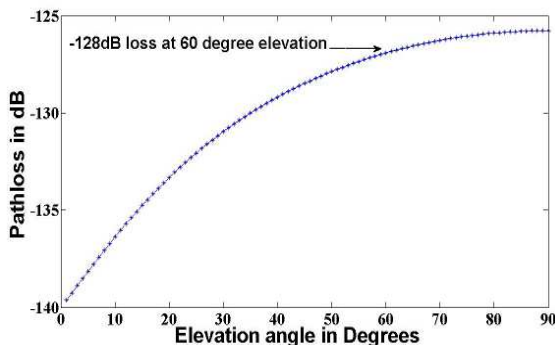


Figure 2: Path Loss vs Elevation

The antenna radiation pattern shows a variation of antenna gain across the space. The received signal strength, being related to the transmitter antenna gain, depends on the region of radiation pattern pointed to by the ground station antenna.⁹ Hence, to attain desired link quality, the antenna should be designed with a radiation pattern profile such that the gain as seen by ground station at 60 degrees elevation corresponds to the system requirement of 6.5dB and hence the beam width requirement of antenna should be about

60degrees with minimum gain of 6.5dB. This is a fundamental design criteria for the antenna discussed in this paper.

ANTENNA DESIGN

Monopole and patch antennas have found wide application in wireless communication. While patch antennas can have high gain depending on the configuration, monopole antennas have lower gain, but omni-directionality. Patch antennas, being planar, can be integrated easily onto the body of a CubeSat, whereas a CubeSat monopole antenna requires a deployment mechanism. The gains of both patch and monopole antennas can be increased through careful design consideration of antenna packaging. Specifically, the gain of patch and monopole antennas increases with ground plane size.³ Gain also depends on the ground plane shape, as seen in the parabolic corner reflector antenna.³

Given that the CubeSat body and deployable solar panel support structure are metallic, the structure can behave as an extended ground plane or reflector, as in the case of a parabolic corner reflector antenna, to improve the antenna gain.³ Employing this concept, three antenna configurations are designed, developed, and tested:

- 1U and 3U Reflector Antenna with Radiating Monopole.
- Extended Parabolic Reflector Antenna with deployable panels.
- Extended Inclined Ground Patch Antenna.

1U Reflector Antenna with Radiating Monopole

A monopole antenna is the simplest antenna design, consisting of a quarter-wavelength radiating element with a low gain of 1.65dB. This gain can be increased proportionally to a ground plane size increase. Improvement in gain and directionality can also be achieved by placing a reflector behind the monopole as in case of reflector antenna with dipole.³ The distance between the reflector and the antenna defines the impedance and gain. The distance is maintained at about 0.2λ as in case of Yagi-Uda antenna.³ For a 1U CubeSat, the dimension of each side is limited to 10cm x 10cm. Hence the ground and reflector sizes are constrained to the same. Designing the metallic solar panel support structure to act as a reflector and using the body of the CubeSat as ground, a monopole reflector antenna with a monopole as radiation element can be constructed. This design differs from a dipole with reflector as in Yagi-Uda antenna.³ Length of the monopole-radiating element is a quarter wavelength at S-band 2.3GHz frequency, which equates to about 3cm.

The antenna is placed at the ground plane center as shown in Figure 3. The distance between the reflector and antenna is a quarter wavelength, or 3cm. This distance is adjusted such that the antenna input impedance is close to the monopole input impedance, of about 40 ohms, to obtain reflection coefficient of less than -10dB such that the loss due to impedance mismatch is minimized. ANSYS HFSS simulation configuration of the antenna, along with the appropriate dimensions, is shown in Figure 3. Figure 5 shows a computer aided design (CAD) model of the antenna setup used for evaluating the 1U CubeSat monopole performance.

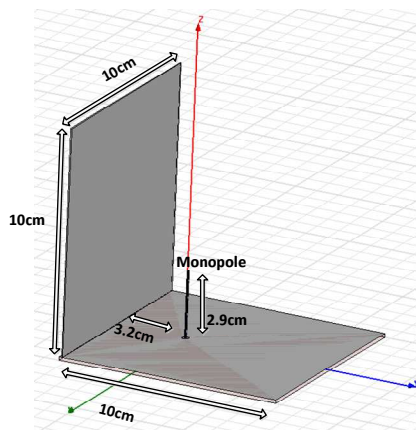


Figure 3: Simulation Setup of 1U Reflector Antenna with Radiating Monopole



Figure 4: Physical Model of 1U Reflector Antenna with Radiating Monopole

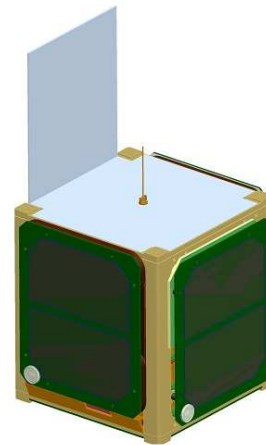


Figure 5: CAD Model of 1U Reflector Antenna with Radiating Monopole

The 2D and 3D radiation pattern, as obtained from ANSYS HFSS, are shown in Figure 6 and Figure 7, respectively. It is observed that the gain of this antenna configuration with the reflector is about 7.5dB with 6.5dB gain at 30 degrees, thus providing the corresponding gain at elevation of 60 degrees. The corresponding reflection coefficient plots as simulated with ANSYS HFSS and measured using VNA are shown in Figure 8. It is noticed that the simulation and measurement results are in good agreement with the minimum reflection coefficient at 2.3GHz, which is -20dB. The impedance of the antenna is measured to be about 42ohms.

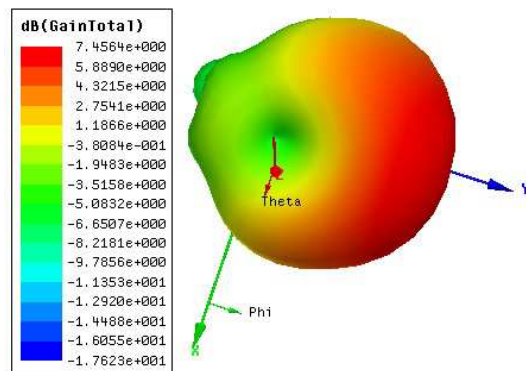


Figure 6: 3D Radiation Pattern Simulation Result for 1U Reflector Antenna with Radiating Monopole

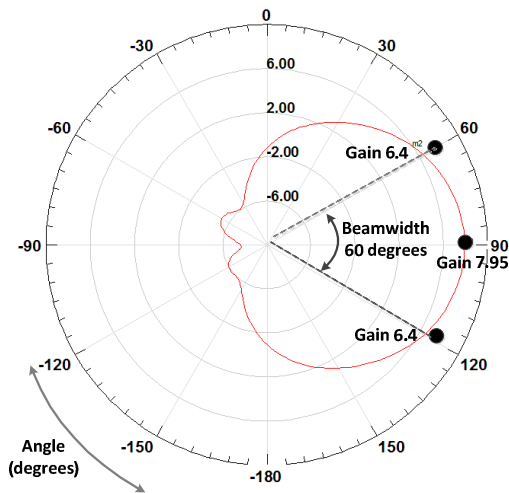


Figure 7: 2D Radiation Pattern Simulation Result for 1U Reflector Antenna with Radiating Monopole

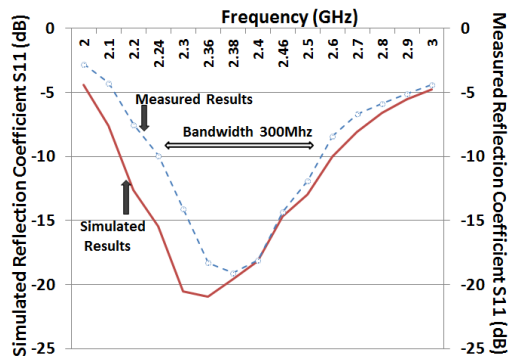


Figure 8: Simulation and Measurement Results of Reflection Coefficient for 1U Reflector Antenna with Radiating Monopole

The 1U CubeSat model discussed up to this point has served as a proof of concept for the concept of using deployable structures for improved gain. The following designs show the extension of the lessons learned from the 1U model to the more capable 3U form factor utilizing deployable panels.

3U Monopole with Deployable Reflector Structure

The 3U monopole with reflector is shown with dimensions in Figure 9 and with the full structure in Figure 10. Similar to the 1U design, the monopole is placed at the center of one of the long faces at about 3.2cm from the panel reflector to obtain a good impedance matching at 2.3GHz.

The simulation results for 3D radiation pattern are shown in Figure 11 with corresponding 2D radiation pattern of Figure 12 show a peak gain of 8.6dB with 6.5dB beam width at 90 degrees. This observed gain is

much more than the required 60-degree beam width. Hence, the 3U configuration of reflector antenna with monopole has marked improvement in ground coverage and gain.

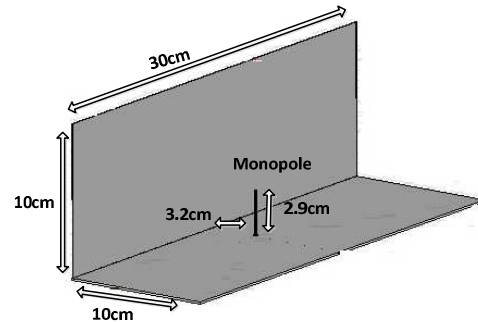


Figure 9: Simulation Setup of Reflector Antenna with Radiating Monopole

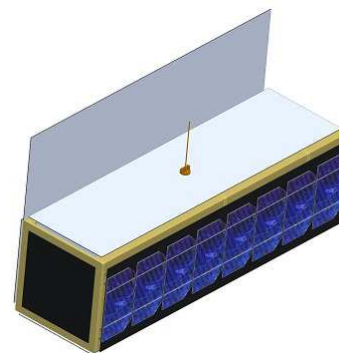


Figure 10: CAD Model of 3U Reflector Antenna with Radiating Monopole

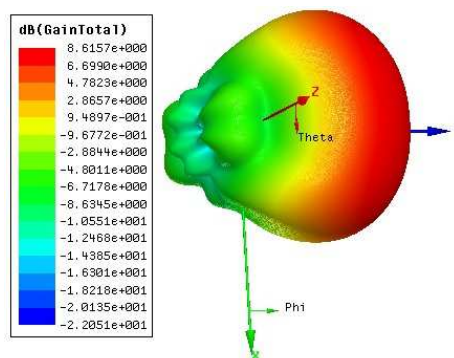


Figure 11: 3D Radiation Pattern Simulation Result for 3U Reflector Antenna with Radiating Monopole

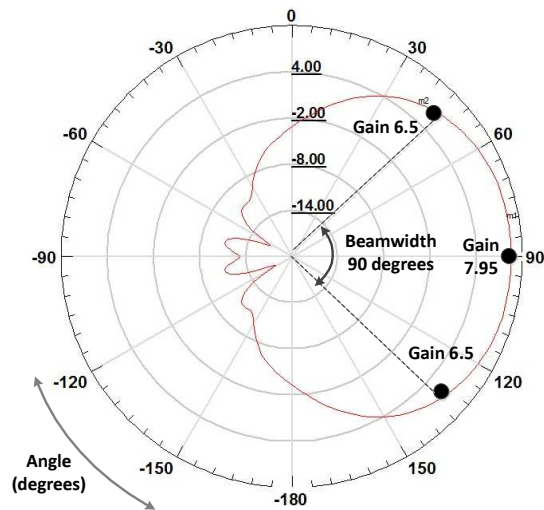


Figure 12: 2D Radiation Pattern Simulation Result for 3U CubeSat Setup of Reflector Antenna with Radiating Monopole

Monopole with Parabolic Reflector

A parabolic reflector antenna can also be designed for the case where it is not possible to have deployable panels. In this case, the reflector is packaged into the body of the 3U CubeSat. The monopole with rectangular reflector, discussed in previous section, can be modified to have a parabolic reflector similar to a parabolic corner reflector used with dipole antennas. Locus of parabolic reflector is governed by ³

$$y = \frac{x^2}{0.8\lambda} \quad (8)$$

The monopole antenna, having a quarter wavelength of about 2.8cm and operating at 2.3GHz, is placed at a distance of about quarter wavelength to maximize the gain and to improve the impedance matching. The monopole antenna is positioned such that the impedance of the antenna provides a reflection coefficient of less than -10dB and bandwidth greater than 10MHz. Figure 13 and 14 show the configuration of parabolic reflector antenna with monopole. From Fig. 15 the radiation pattern as obtained from ANSYS HFSS simulation at 2.3GHz shows a gain of 7.7dB. Since the gain is proportional to the reflector area, it can be further improved by increasing size of the reflector. This antenna design can be accommodated by both the 3U and 1U CubeSat form factor.

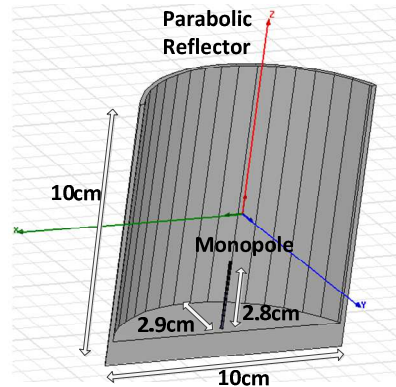


Figure 13: Simulation Setup of Monopole with Parabolic Reflector



Figure 14: Physical Model for Monopole with Parabolic Reflector

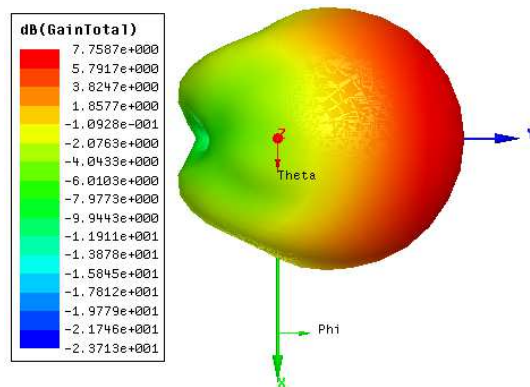


Figure 15: 3D Radiation Pattern Simulation Result for 3U with Parabolic Reflector at 2.3GHz

3U Parabolic Antenna with Deployable Extended Reflector

The previous parabolic reflector antenna gain can be further improved with deployable solar panels such that

the metallic solar panel support structures act as extensions of the parabolic reflector. The parabolic reflector antenna is placed in the middle of the longest side of 3U CubeSat containing a deployable solar panel. The parabolic structure is embedded onto the body of CubeSat, such that the body, as well as the deployable solar panel support structure, acts as an extension of the reflector, thus improving the antenna gain. Additionally, inclining the solar panel leads to further gain improvement. A simulation setup of the antenna on a 3U CubeSat with deployable panels and its associated CAD and physical setup are shown in Figures 16, 17 and 18, respectively.

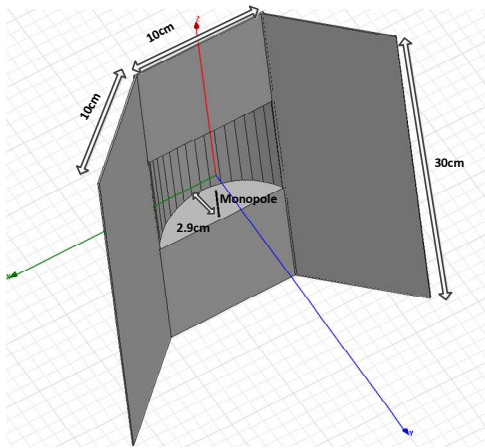


Figure 16: Simulation Setup of 3U Parabolic Antenna with Deployable Extended Reflector

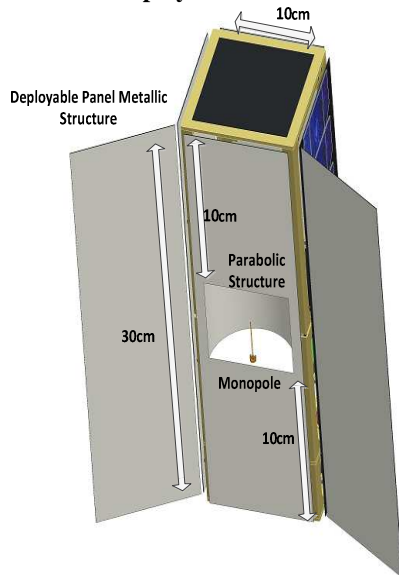


Figure 17: CAD Model of 3U Parabolic Antenna with Deployable Extended Reflector

A physical model of this antenna configuration, shown in Figure 18, has been developed to evaluate its performance. The HFSS simulation results of Figure 19 and Figure 20, shows a gain of 9.7dB with 6.5dB gain beam width of about 74 degrees, which is more than design requirement. The reflection coefficient computed from ANSYS HFSS simulation and measured using VNA show good agreement as depicted in Figure 21. The reflection coefficient plot shows a -10dB bandwidth of more than 10MHz with a minimum of -24dB reflection coefficient at 2.3GHz. Note, the impedance of the antenna is about 42ohms.



Figure 18: Physical Model of 3U Parabolic Antenna with Deployable Extended Reflector

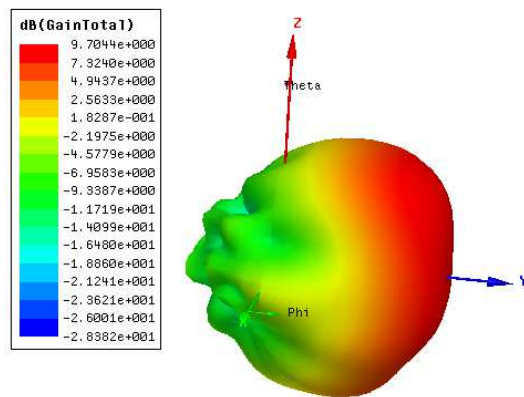


Figure 19: 3D Radiation Pattern Simulation Result for 3U Parabolic Antenna with Deployable Extended Reflector

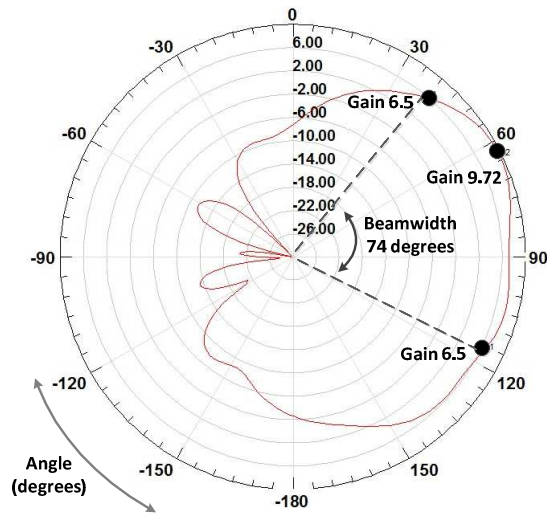


Figure 20: 2D Radiation Pattern Simulation Result for 3U Parabolic Antenna with Deployable Extended Reflector

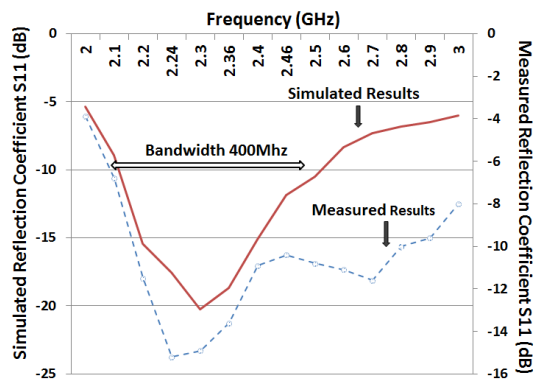


Figure 21: Simulation and Measurement Results of Reflection Coefficient

Thus, placing the parabolic antenna in the center of one of the sides with deployable panels provides an additional gain of more than 2dB above the gain of parabolic reflector with monopole without deployable panels and an improvement in coverage through a wider beam width. The insight gained from this design can be extended in the development of new designs by placing other antenna types at the center of a 3U CubeSat face to improve gain. Examples include patch and patch array antennas.

3U Extended Inclined Ground Patch Antenna

In the previous section it was concluded that placing the antenna in center of one of the 3U CubeSat sides with deployable panels could improve the gain. This concept can be extended to gain improvement of patch antennas.

The metallic body of the satellite can be used as an extension of the patch antenna ground, which leads to an increase in gain due to increased ground plane size. Patch antennas with lower gains, like annular ring patch antennas with gain of 4.7dB, can be made to have more than 3dB gain improvement through such configuration.

The annular-ring patch antenna, shown in Figure 22, consists of a ring-like configuration of copper trace on a substrate, which is assumed to be Rogers5880 with 1.59cm thickness. The ring is designed such that the circumference of the center circle of the ring is approximately a wavelength corresponding to a frequency of 2.4GHz.¹¹ Position of the antenna feed is adjusted to obtain 50 ohm input impedance. Figure 23 shows that annular-ring patch antenna, without deployable structures, has a gain of 4.79dB.

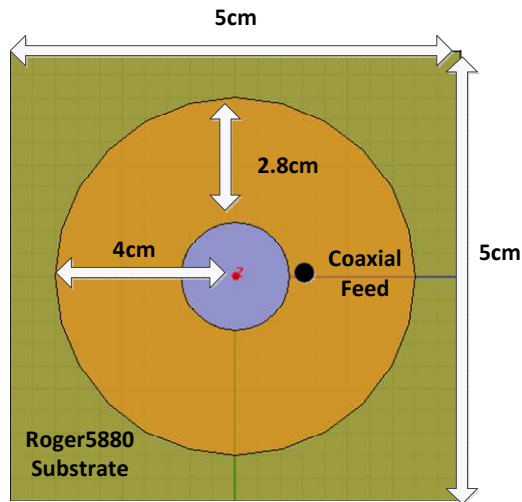


Figure 22: S-Band Annular Ring Patch Antenna Design

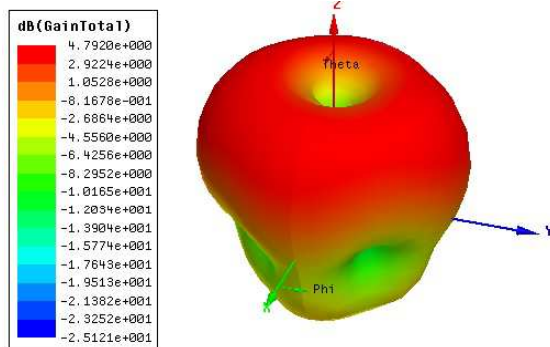


Figure 23: Simulated Annular Ring Patch Antenna 3D Radiation Pattern

3U Extended Inclined Ground Patch Antenna with Deployable Panels

The gain of the annular-ring patch antenna can be increased by placing the antenna in the center of one of the sides of the 3U CubeSat with metallic deployable solar panels. The packaging is similar to the configuration used in Figure 17. Figure 24 shows the antenna setup on the 3U CubeSat. The fabricated antenna with the test model of 3U CubeSat configuration is as shown in Figure 25.

Figures 25 and 26 show the 3D and 2D radiation pattern as obtained from simulation. It is observed that by using deployable panels, the gain is 7.9dB, which is a 3dB gain improvement on the annular-ring patch antenna gain of 4.5dB without deployable panels. Additionally, the antenna has a 6.5dB beam width of 56 degrees that is closer to the required 60 degrees beam width. The concept can be extended to other patch antennas like rectangular patch antenna.

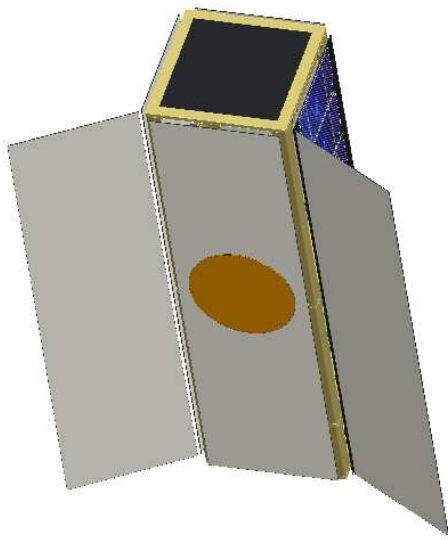


Figure 24: CAD Model of 3U Annular Ring Patch Antenna



Figure 25: Physical Model of Annular Ring Patch Antenna

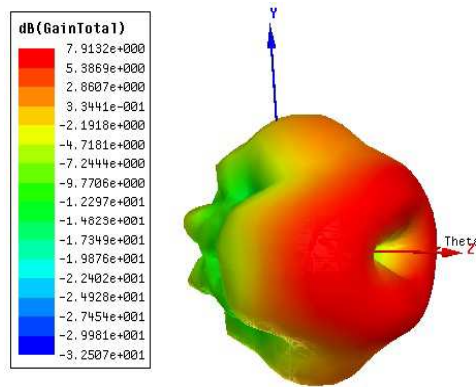


Figure 26: Simulated 3D Radiation Pattern of Annular Ring Patch Antenna on 3U CubeSat

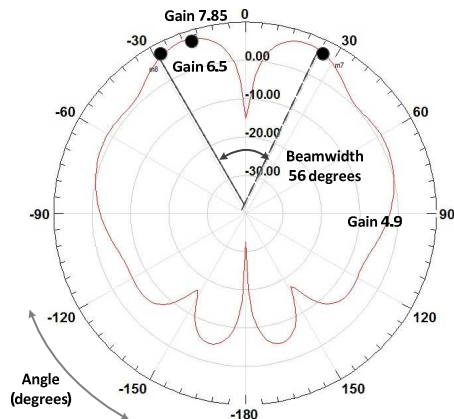


Figure 27: Simulated 2D Radiation Pattern of Annular Ring Patch Antenna on 3U CubeSat

Antenna Measurement Testbed

Up to this point, all of the designs have been verified through simulation. All of the presented antenna designs developed were evaluated with a testbed

consisting of a transceiver, microcontroller and commercial 7dBi gain patch antenna. It consists of transmitter setup with software embedded on an MSP430F2012 microcontroller that communicates with an Atmel At86rf212 S-band transceiver to transmit packets with output power of 0dBm through a commercially available patch antenna with 7dBi gain. Packets are received and evaluated for the Received Signal Strength Indicator (RSSI) to verify the gain improvement over the 7dBi gain antenna. The setup is as in Figure 28. Table 1 lists the RSSI values obtained with a reference antenna each tested antenna. It can be observed that the received signal strength for the antennas shows improvement in gain comparable to the antenna gain improvement over 7dBi.

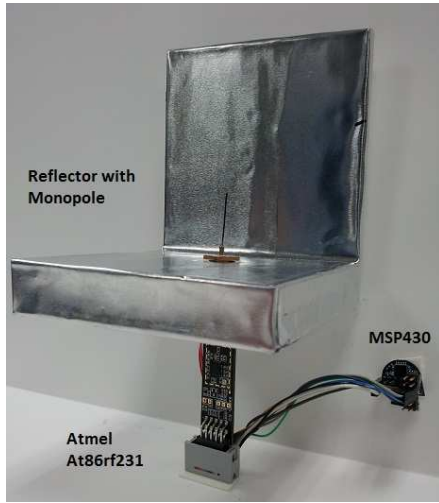


Figure 28: RSSI Evaluation setup for S-band Antenna

Table 1: Style Specifications

Antenna	RSSI Improvement of 7dBi gain antenna
1U reflector with monopole	1dB
3U reflector with monopole	2dB
3U Parabolic reflector with monopole	3dB
3U Annular patch antenna	1dB

Antenna Configurations Attitude Stability

Multiple antennas were designed, developed, and tested for the purpose of gain improvement with the intention of implementation on orbit. One important consideration for the implementation of these antennas is how they impact the satellite's attitude stability. There are two aspects that must be considered:

- Operating attitude of the antenna design

➤ Gravity-gradient stabilized attitude

The operating attitude is determined by the directionality of the antenna and the orientation of the antenna relative to the spacecraft body. Gravity-gradient torque is applied to non-uniform inertia satellites, which acts to align the minimum principal axis with the gravity vector. If the operating attitude of the antenna and the gravity-gradient stabilized attitude conflict, then an active attitude control is necessary to communicate with each of the directional antenna design.

Without loss of generality, the principal axes of the 3U CubeSat will be assumed to align with the standard body-fixed axes such that the z-axis is parallel to the longitudinal body-fixed axis pointing out of one of the 10cm x 10cm faces. The x- and y-axis point out of the 30cm x 10cm satellite faces and complete a right-hand triad to form a basis.

The gravity gradient torque acting on the spacecraft is

$$\tau_{GG} = 3 \frac{\mu}{r^3} \hat{c} \times (J \cdot \hat{c}),$$

where μ is Earth's gravitational parameter, r is the magnitude of the position vector, \hat{c} is the nadir-pointing direction and J is the inertia tensor. Given the aforementioned principal basis, then the moment of inertia tensor coordinated in body coordinates about the center of mass is

$$J_c = \begin{bmatrix} J_{xx} & 0 & 0 \\ 0 & J_{yy} & 0 \\ 0 & 0 & J_{zz} \end{bmatrix},$$

where the components of the inertia matrix are ordered such that

$$J_{zz} < J_{yy} < J_{xx}.$$

Since the z-axis is the minimum moment of inertia axis for a 3U CubeSat, it is well known that under this condition the satellite will reach a gravity-gradient stabilized attitude pointing the z-axis along the gravity vector. However, this attitude is contrary to the antenna designs presented in this paper. Therefore, the main objective of the attitude control system is to ensure that the attitude for communication is maintained when communication is necessary.

There are two possible attitude scenarios that exist for utilization of the communication system:

- The satellite is operating as a dedicated downlink and always needs to have the directional antenna pointing within a boresight cone of the nadir direction
- The satellite has other attitude objectives, based on a primary mission, such as image capture, that possibly conflicts with the attitude necessary to communicate with the directional antenna

Under the conditions of the first scenario, passive attitude control is sufficient to maintain required attitude. One such solution is to utilize a strong enough permanent magnet with hysteresis to overcome the gravity-gradient torque and align the antenna boresight direction with nadir by creating an appropriate magnetic moment.

In the second scenario, active 3-axis attitude control is necessary. At a minimum, the attitude control system must be capable of producing a torque greater than the gravity gradient torque. Depending on the slew-rate and precision requirements, angular momentum exchange devices, such as reaction wheels and control moment gyroscopes, exist for overcoming gravity-gradient effects to provide full 3-axis attitude control. Given this control, the satellite can then reorient between the attitude for image capture and downlink.

Drag and Orbital Lifetime Considerations

A significant advantage of the proposed antenna designs is that their communication attitude requirements result in increased orbital lifetime. Since each of the designs operates with the 3U longitudinal axis (z-axis) parallel to the velocity vector, the drag area is minimized. Minimizing area is important because orbital decay is a direct result of delta-v loss due to the drag acceleration and other acceleration perturbations. However, as discussed in the previous section, this does come at the cost necessitating a passive or active attitude control system to overcome gravity-gradient effects.

Conclusion

Several antenna concepts have been developed to achieve high gain in a space constrained CubeSat. The antenna models are developed, simulated, and tested with respect to gain performance. These antennas designs were packaged for 1U and 3U CubeSat platforms. Each antenna was required to have a beam width of greater than 60 degrees, bandwidth greater than 10MHz, and gain greater than 7dB. Simulation and test measurements verified the performance of the antenna configuration. A link budget analysis was performed to estimate the gain requirements for based

on sensitivity requirements such that the maximum transmit power is limited to 1W that is representative of the standard power consumption of available CubeSat communication subsystems. The antennas were also tested to evaluate the improvement in received signal strength using an Atmel transceiver and software running on an MSP430f2012 microcontroller. Although these designs apply to linear polarized antennas, the concepts presented can be extended to circular polarized antennas, like crossed dipoles, instead of monopole configurations to further improve link quality.

Acknowledgments

The work presented here could not have been completed without the support of all the members of Space Systems Group at the University of Florida. We would also like to acknowledge the support of Kelly Jenkins and Malathy Elumalai, the engineers from the McKnight Brain Institute at the University of Florida, for assisting us with antenna measurements.

References

1. Cason, K., Shirvante, V., Johnson, S., Patankar, K. and N. Fitz-Coy, "A Nano-Satellite Constellation for advanced Fire Identification", 10th AIAA Reinventing Space Conference, Los Angeles, CA, May 2012.
2. Lutz, E., Werner, M. and A. Jahn, Satellite systems for personal and broadband communications, Springer, New York, 2000.
3. Balanis, C. A., Antenna Theory: Analysis and Design, John Wiley & Sons, Publication, Hoboken NJ, 2005.
4. Eskelinen, P., Introduction to RF equipment and system design, Artech House, Norwood MA, 2004.
5. Gomez, M.J., Satellite broadcast systems engineering, Artech House, Norwood MA, 2002.
6. Seybold, S.J., Introduction to RF propagation, John Wiley & Sons, Hoboken NJ, 2003.
7. Richharia, M., Satellite communication systems: Design principles, McMillan Press Ltd, 1999.
8. Bouwmeester, J., Gill, E., Sundaramoorthy, P. and H. Kuiper, "Concept Study of A LEO constellation of nanosatellites for near real time optical remote sensing", 63rd International Astronautical Congress, Naples, Italy, October 2012.
9. Ho, C., Katak, A., Slobin, S. and D. Marobito," Link Analysis of a Telecommunication System on Earth, in Geostationary Orbit, and at the

Moon: Atmospheric Attenuation and Noise Temperature Affects”, IPN Progress Report 42-168, February, 2007.

10. Khotso, P.A., Lehmensiek, R. and R. R. van Zyl, “Comparison of the communication time of a high gain versus a low gain monopole-like low profile antenna on a 3-unit CubeSat”, IEEE AFRICON, vol., no., ppl.1-4, Livingstone, Zambia, September, 2011.
11. Kumar, G. and K.P. Ray, Broadband Microstrip Antennas, Artech House, Norwood MA, 2003.